Nat. Volatiles & Essent. Oils, 2021; 8(4): 14506-14529

Spatial Filterative Stochastic Gene Optimized Feature Selection Based Deep Jaccard Regressive Squeezenet Learning For Land Cover Change Detection With Satellite Images

Mrs A. Jensila Smile[1] , Dr (Mrs) C. Immaculate Mary[2]

Part Time Ph.D. Research Scholar & Asst. Professor in Computer Science (SF), Sri Sarada College for Women (Autonomous), Salem-636 016.[1]

H.O.D & Associate Professor, Dept. of Computer Science, Sri Sarada College for Women (Autonomous), Salem-636 016.[2]

Abstract-Change detection is a significant process in satellite surveillance. With the availability of satellite images of a certain geographical area captured in dissimilar time instances, change detection is considered a tough task. Land cover classification of satellite images has been a very biggest area since the amount of information acquired by satellite imaging systems is more. Satellite images reveal spatial and/or temporal information's in which the conventional machine learning algorithms fail to perform well for accurate change detection. To improve the land cover change detection rate, a novel technique called Spatial Filterized Stochastic Gene Optimization-based Deep Jaccard Regressive Squeezenet Convolutional Structure learning (SFSGO-DJRSCSL) is introduced. The SFSGO-DJRSCSL technique consists of three major processes namely preprocessing, feature selection, and change detection. At first, the input satellite images at a different time are captured from the dataset. After collecting the images, the proposed SFSGO-DJRSCSL starts to perform the preprocessing with the input satellite images captured at a different time. After the preprocessing, the stochastic roulette gene optimization based feature selection is carried out to choose the optimal feature combination for change detection resulting in it reduces time consumption. The extracted features are given to the Deep Jaccard Regressive Squeezenet Convolutional Structure learning to detect the changes between homogeneous images. Jaccard index Regression function is applied to map the features extracted from the two homogeneous images and accurately perform the change detection with a lesser error rate. An experimental assessment of the proposed SFSGO-DJRSCSL technique is carried out using a satellite image dataset. The results are discussed with the different performance metrics such as detection rate, false alarm rate, the detection time for different satellite images.

Keywords-Land Cover Change Detection, satellite images, preprocessing, stochastic roulette gene optimization, Jaccard indexing Regression, Squeezenet Convolutional Structure learning

1. INTRODUCTION

Change detection aims to discover the variation in multi-temporal images of a similar geographic location. Monitoring changes in bi-temporal remotely sensed images are essential to the understanding of land surface changes. The change detection has been widely applied for different applications, such as disaster damage assessment, land cover mapping, and urban expansion investigation, and so on. The conventional techniques are not exactly performed the change detection in high-resolution images. Therefore, deep learning-based change detection methods have been proposed to improve change detection performance.

A deep Siamese Convolutional Multiple-Layers Recurrent Neural Network (SiamCRNN) was introduced in [1] for change detection with multitemporal images. The designed SiamCRNN failed to apply the hyperspectral image and it also not efficient to perform accurate detection with minimum time consumption. A deeply Supervised Image Fusion Network (IFN) was developed in [2] to identify the changes from the satellite images. However, different radiometric corrections were not performed to obtain the quality enhanced image for accurate change detection. Maximum likelihood classifiers (MLC) were introduced in [3] to discover the land cover change detection. However, the performance of the detection rate was not considered.

A Deep Change Vector Analysis (DCVA) was introduced in [4] to discover the changes from multitemporal images that use the convolutional neural network (CNN). However, the designed method failed to achieve the improved performance of change detection. An automatic change detection model was developed in [5] using multi-temporal images with planar-vertical features. However, the model did not sufficiently reduce the false alarm rate.

A Bayesian statistical approach was introduced in [6] for multimodal change detection with the remote sensing image. But the approach failed to deeply analyze the features. A binary feature descriptor-based method was introduced in [7] to perform the change detection using optical satellite images. However, the preprocessing of bitemporal optical satellite images was not performed.

A Hybrid Kohonen Fuzzy C Means sigma classifier was presented in [8] for unsupervised change detection. Though the classifier increases the accuracy, the cancer detection time was not considered. A deep capsule network was introduced in [9] to detect the changes using pixel-level mapping. The designed technique was not utilizing the multi-spectral images and other types of images.

A neuro-fuzzy classifier was developed in [10] that employs the mixed pixel of satellite images using a similarity index. But, the classifier failed to deeply analyze the features to reduce incorrect change detection.

1.1 OUR CONTRIBUTIONS

The main contributions of our SFSGO-DJRSCSL technique are summarized as follows:

- A novel SFSGO-DJRSCSL technique is introduced for accurate change detection using land cover satellite images.

- ❖ To improve the change detection rate, the SFSGO-DJRSCSL technique uses the Deep Jaccard Regressive Squeezenet Convolutional Structure learning. The deep learning architecture analyzes the features in the multiple hidden layers. The Jaccard regression function is applied to map the features based on the similarity value. As a result, the changes are correctly detected in the output layer. This also minimizes the false alarm rate.

- ❖ To reduce change detection time, the SFSGO-DJRSCSL technique performs preprocessing and feature selection as well as extraction. In the preprocessing phase, various corrections are performed such as radiometric correction, atmospheric corrections, topographic correction, and contrast enhancement. This process enhances the image quality and reduces the time consumption of change detection. The stochastic roulette gene optimization technique is also applied for detecting the optimal features and extracting the features for change detection.

- ❖ Finally, Extensive and comparative experiments were conducted to evaluate the quantitative and qualitative analysis based on the different performance metrics

1.2 OUTLINE OF THE PAPER

This paper is structured with five different sections. Section 2 reviews the different change detection methods. Section 3 describes the proposed methodology with a neat diagram. In Section 4, Experiments of the homogeneous images are carried out followed by qualitative and quantitative discussions that are presented with the help of charts and tables. At last, concludes the paper with a discussion in Section 5.

2. RELATED WORKS

A change detection method was developed in [11] based on the hybrid spectral difference (HSD). However, the designed method was failed to identify only the spectral features of individual pixels. A spatiotemporal multi-resolution segmentation (ST-MRS) model was developed in [12]. However, it failed to focus on feature extraction, classification, and change detection.

Dempster-Shafer theory (D-S) was introduced in [13] for urban change detection. The designed method increases the detection and reduces the false alarm but the time consumption was not reduced. A new recurrent convolutional neural network (ReCNN) was developed in [14] to accurately learn a joint spectral–spatial-temporal feature for change detection. The architecture design failed to work with a large amount of unlabeled data.

A conditional generative adversarial network (cGAN) was introduced in [15] for change detection. However, the higher detection rate with minimum time consumption was not achieved. Asymmetric convolutional coupling network (SCCN) was presented in [16] for change detection based on the varied images. But the network failed to handle more than two heterogeneous images of dissimilar types.

A bipartite differential neural network (BDNN) based image change detection was performed in [17] by extracting the holistic features from the input images. The method was not reduced the incorrect detection. A shape-aware siamese convolutional network (SASCNet) was developed in [18] to concurrently combine the dissimilar information for change detection.

A kernel-based change detection algorithm was developed in [19] to increase true positives and reduce false positives. However, the designed algorithm failed to reduce computational time consumption. A new SAR image change detection technique was introduced in [20] but accurately extracting saliency maps from saliency regions and discovering the more detailed changes were not performed.

3. METHODOLOGY

With the rapid growth of earth observation technology, very-high-resolution images were collected from the various satellite sensors which were significantly used for change detection. A remote sensing image provides the macro view of earth observation and it comprises the Multitemporal images which covering a similar scene to expose the dynamic environmental changes in the ground. A multitemporal image is an image captured for a different time. Therefore, the change detection technology uses multitemporal images for identifying the differences in the state of an object at different times. To accurately detect the changes in similar satellite images, a novel SFSGO-DJRSCSL technique is introduced. The architecture of the deep learning-based approach is illustrated in figure 1.

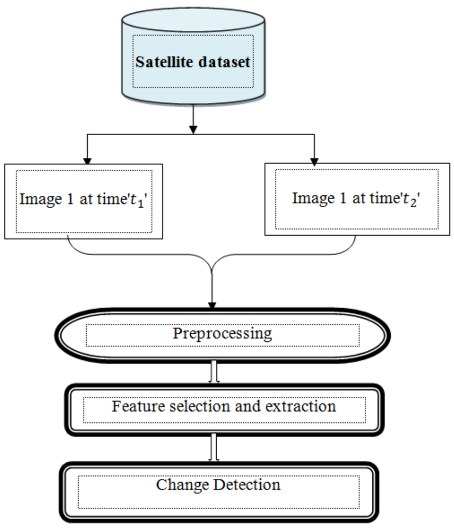

FIGURE 1: ARCHITECTURE OF THE PROPOSAL SFSGO-DJRSCSL TECHNIQUE

Figure 1 illustrates the architecture of the proposal SFSGO-DJRSCSL technique in which three major processes are carried out to obtain a higher detection rate with minimum time consumption. The input satellite land images $L_1, \quad L2, L_3 \dots\dots L_n$ at different times are collected from the database. The collected noisy images are applied to the preprocessing stage to obtain the quality enhanced input image for accurate change detection. The proposed SFSGO-DJRSCSL technique performs optimal feature selection and spatial feature extraction process using stochastic roulette gene optimization. Finally, the change detection is performed with the extracted features using Deep Jaccard Regressive Squeezenet Convolutional Structure learning. The detailed processes of our proposed SFSGO-DJRSCSL technique are described in the following subsections given below.

3.1 PREPROCESSING

The first step of our proposed SFSGO-DJRSCSL technique is preprocessing which consists of radiometric correction,Apparent reflectance method based Atmospheric corrections, Gamma method based Topographic correction, Linear contrast Stretching based contrast enhancement. These processes are explained in given below.

Radiometric correction is adopted to remove the radiometric difference between multitemporal images caused by dissimilar sun angles, light intensity, and atmospheric conditions. The Radiometric correction is done by the normalization of the input satellite image into zero mean and unit deviation. Radiometric normalization is the process of conversion of all sensor values obtained from the images into a common scale. Let us consider the input satellite image taken at a time 't_1' is $L_1\ (t_1)$ and time 't_2' is $L_1\ (t_2)$. The input images are considered in the two-dimensional spectral bands and pixels are denoted as $p_i \in p_{i1}, p_{i2}, p_{i3,\dots\dots} \ p_{im}, p_j \in p_{j1}, p_{j2}, p_{j3,\dots\dots} p_{jn},$ Where, p_i, p_j denotes a pixel in two-dimensional spectral bands. The relative radiometric normalization of these two pixels of the satellite images are represented as given below,

$$N\ (p_i) = \frac{(p_{im} - \mu_{p_{im}})}{d_{p_{im}}} \quad (1)$$

$$N\ (p_j) = \frac{(p_{jn} - \mu_{p_{jn}})}{d_{p_{jn}}} \quad (2)$$

From (1), (2), $N\ (p_i)$ and $N\ (p_j)$ denotes a normalization of the pixels vectors p_i and p_j, $\mu_{p_{im}}$, $d_{p_{im}}$ denotes a mean and deviation of the image 'i'. $\mu_{p_{jn}}$ and $d_{p_{jn}}$ indicate a mean and deviation of the image 'j'. p_{im} denotes an 'm' number of pixels in input image 'i', p_{jn} denotes an 'n' number of pixels in image 'j'. As a result of radiometric normalization, the various dimensions of the input images are obtained in a similar range.

APPARENT REFLECTANCE METHOD BASED ATMOSPHERIC CORRECTIONS

Atmospheric correction is one of the preprocessing steps which help to remove the effects of the atmosphere on the reflectance values of land images captured from the satellite. The Apparent reflectance method is applied to perform the atmospheric correction. This approach corrects the effects originated by solar irradiance and solar zenith angle and removes the effects of atmospheric scattering and absorption. The corrections are done by using the following expression,

$$r_\lambda = \frac{\pi * v^2 * R_{\lambda_S}}{(R_{\lambda_{SX}} * \cos(\theta_Z))} \quad (3)$$

Where r_λ indicates a surface reflectance, π denotes a constant π =3.14, R_{λ_s} indicates a Spectral radiance at the sensor's aperture, $R_{\lambda_{ex}}$ denotes an Exo-atmospheric solar spectral irradiance, $\cos \theta_Z$ indicates a solar zenith angle, λ indicates a Wavelength, 'v 'symbolizes the distance between earth and sun (unit: Astronomical unit (AU)). The Spectral radiance at the sensor's aperture'R_{λ_s}' is expressed as follows,

$$R_{\lambda_s} = dn_{cl} * G_\lambda + B_\lambda \quad (4)$$

Where dn_{cl} indicates a quantized calibrated pixel value, G_λ indicates a Radiometric gain, B_λ denotes a Radiometric bias. As a result, atmospheric corrections are performed effectively.

GAMMA METHOD BASED TOPOGRAPHIC CORRECTION

A topographic correction is also known as a terrain correction which helps to remove the effects of topography. High spatial resolution satellite images in rough areas often contain large terrain effects, therefore the topographic correction is also a basic step of pre-processing for rough areas. A Topographic correction is done by applying the gamma method.

$$T_h = \rho_t * \left[\frac{\cos\theta_d + \cos\theta_b}{\cos\alpha + \cos\alpha_b}\right] \quad (5)$$

Where, T_h indicates a horizontal surface, ρ_t denotes a reflectance of an inclined (terrain), θ_d denotes a terrain slop, θ_b denotes a sensor view angle on flat terrain, α_b denotes a sensor view angle on inclined terrain, α denotes a terrain angle.

LINEAR CONTRAST STRETCHING BASED CONTRAST ENHANCEMENT

The satellite images are captured through the sensors and it may have blurred or low contrast. The contrast enhancement technique increases the brightness values so that the image quality is efficiently enhanced in the desired manner. The Linear contrast Stretch algorithm is used to obtain the contrast-enhanced image.

In general, image contrast is enhanced by distributing the range of color values i.e. RGB (red, green, blue) to construct with the use of all possible pixel values. By applying the linear contrast Stretching method, the contrast enhancement is obtained as follows,

$$O_{RGB}\ (x, y) = 255 * \left\{\frac{L_{RGB}\,(x,y) - \varphi_{min}}{\varphi_{max} - \varphi_{min}}\right\} \quad (6)$$

From (6), $O_{RGB}\ (x, y)$ denotes a contrast-enhanced RGB value of pixels, $L_{RGB}\ (x, y)$ denotes an RGB value of pixels in an original input image, φ_{min} denotes a minimum pixel value for each RGB component i.e. 0, φ_{max} denotes a maximum pixel value for each RGB component i.e. 255. By using (6), the image contrast is enhanced and obtains the quality improved image for accurate change detection with minimum error.

SPATIAL FILTERING

Spatial filtering is the process of partitioning the image into its constituent spatial frequencies and selectively altering certain spatial frequencies to emphasize some image features. This technique is done to increases the ability to discriminate in detail. A Linear spatial filtering technique is applied directly to pixels of an input satellite image. In the filtering process, the mask is usually considered and it is moved on the image such that the center of the mask traverses all image pixels.

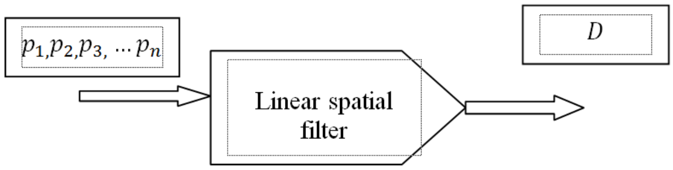

FIGURE 2: LINEAR SPATIAL FILTERING

Figure 2 demonstrates the linear spatial filtering to change the (spatial) frequencies of images with the help of a filter mask with the size of $* k$. Let us consider the 3*3 filter mask which comprises the filter coefficients $\omega_1, \omega_2, \omega_3, \dots \omega_n$. These filter masks moving the pixels to pixels of the input image $p_1, p_2, p_3, \dots p_n$. Therefore, the output filtered results are obtained as follows,

$$D = \sum_{i=1}^{n} \omega_i * p_i \quad (7)$$

Where D denotes a filtered output. This helps to remove the unwanted noisy pixels in an image.

// Algorithm 1: Image preprocessing
Input : Dataset, satellite images $L_1, L_2, L_3 \dots.. L_n$ **Output** : Preprocessed image
Begin **1.** **For each** image $L_i\ (t_1)$ and is $L_i\ (t_2)$ **2.** Perform Radiometric normalization using (1) (2) **3.** Perform Atmospheric corrections using (3) (4) **4.** Perform Topographic correction using (5) **5.** Perform Contrast enhancement $O_{RGB}\ (x, y)$ **6.** Apply linear spatial filtering 'D' **7.** Obtain smoothed image **8.** **End for**

Algorithm 1 given above illustrates the preprocessing stages of the proposed SFSGO-DJRSCSL technique. The input satellite images are collected from the database. For each input image, radiometric normalization is performed to change the scale of the input image into mean and variance. Followed by, the atmospheric correction is performed using the apparent reflectance method and topographic correction is carried out using the Gamma method. Followed by, the linear contrast Stretching method is applied to enhance the image contrast to performing accurate change detection with minimum time. Finally, the spatial filtering process is carried out to smooth the images.

3.2 STOCHASTIC ROULETTE GENE OPTIMIZATION-BASED FEATURE DETECTION

After preprocessing, the feature detection is performed using stochastic roulette gene optimization to find the survival of the fittest features. The satellite images are collected and stored with a large volume of the database. In such a situation, a stochastic genetic algorithm is mainly used to adaptively search for the best feature combination in feature space and to select optimal features.

A stochastic roulette gene optimizationis a bio-inspired meta-heuristic technique and it is often developed to resolve search and optimization problems. It can evaluate the entire input space and generates good solutions in a reasonable time. Here, stochastic optimization is the optimization that generates and uses random objective functions or random constraints in the formulation of the optimization. The features of the remote sensing image are texture (t), intensity(I), and color (c) to generate a feature vector. Based on the features, the combinations are created randomly to generate the initial population in the search space.

$W_i = C_1, C, C_3, \dots . C_m$ (8)

Where, $W_i$denotes a feature combination $C_1, C, C_3, \dots . C_m i.e\ C_1 = (t, I, c)$, $C_2 = (t, c)$, $C_3 = (t, I)$ and so on. Among these multiple combinations, the optimal one is selected for accurate change detection with minimum time. Then the fitness is computed for each combination to find the optimal one.

$F = \arg\min E$ (9)

Where$F$ denotes a fitness, $\arg\min$ denotes an argument of the minimum function, E indicates an error. Based on the fitness computation, the optimal fittest feature combination is selected. If the fitness criterion is not satisfied, then the genetic operators such as roulette wheel selection, two-point crossovers, and flip bit mutation are performed to attain the optimal feature combination.

3.2.1 ROULETTE WHEEL SELECTION

Roulette wheel selection is applied in the proposed optimization technique for selecting the best individual from the population-based on fitness. Let us consider a circular wheel and it is partitioned into different segments. Each segment has a feature combination. The selection of the best individual is revealed in figure 3.

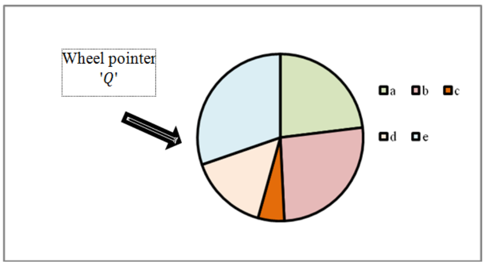

FIGURE 3: ROULETTE WHEEL BASED SELECTION

Figure 3 given above illustrates the roulette wheel based selection using pointer 'Q'. From the figure, the different segments are indicated by the different colors which indicate a fitness value of the different individuals i.e. feature combination. Then the roulette wheel is rotated. The individual which comes in front of the wheel pointer is chosen and it has higher fitness than the other. The probability of selecting the best individuals from the population is obtained as follows,

$$P_r = \frac{F_i}{\sum_{j=1}^{m} F_j} \quad (10)$$

Where, P_r indicates a selection probability, F_i signifies a fitness of individual 'i' in the population 'j', 'n' denotes the number of individuals in the population. Based on the above probability, individuals with higher probability are selected for recombination.

3.2.2 TWO-POINT CROSSOVER

The two-point crossover is a genetic operator to integrate the genetic information of two parent's chromosomes and create offspring. It is a one-way function and generates novel solutions from an existing population. Let us consider the two parents' chromosomes with the binary representation of the individual. The proposed technique uses two-point crossovers for generating offspring. The binary representation of the chromosomes are $A = b_1, b_2, b_3 \ldots . b_n$ and $B = A = s_1, s_2, s_3 \ldots . s_n$. Then the offspring is generated as shown in figure 4.

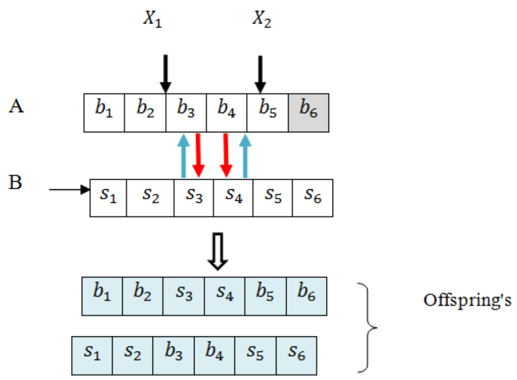

FIGURE 4: TWO-POINT CROSSOVERS

As shown in figure 4, the two-point crossover is illustrated to obtain the offspring's through the recombination process. The two offsprings are generated based on two cross points X_1 and X_2 are shown in figure 4. Hence it is called a two-point crossover. Based on the crossover results, the two-parent chromosomes are recombined and to generate new off-springs. After the generation, the string length of the obtained offspring is equal to the total string length of initial parent chromosomes.

3.2.3 FLIP BIT MUTATION

Flip Bit Mutation is another genetic operator in the optimization technique that helps to preserve the genetic diversity from one generation to the next. The Flip Bit Mutation is the process of changing one or more genetic values (i.e. binary representation) in a chromosome from the newly generated offspring. As a result, the algorithm obtains a better solution by using mutation. The proposed technique uses flip bit mutation for randomly changing the bit i.e. '1' to '0' and vice versa at a random position.

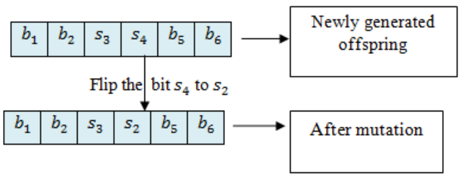

FIGURE 5: FLIP BIT MUTATION

Figure 5, demonstrates the flip bit mutation of the offspring value of string 's_4' is randomly changed with the exact string of 's_2 '. As a result, new offspring are generated and a previously selected individual gets changed with a new one. Followed by, the fitness criterion is verified again to obtain optimal fittest combination features. This process is stopped until the iteration gets reached.

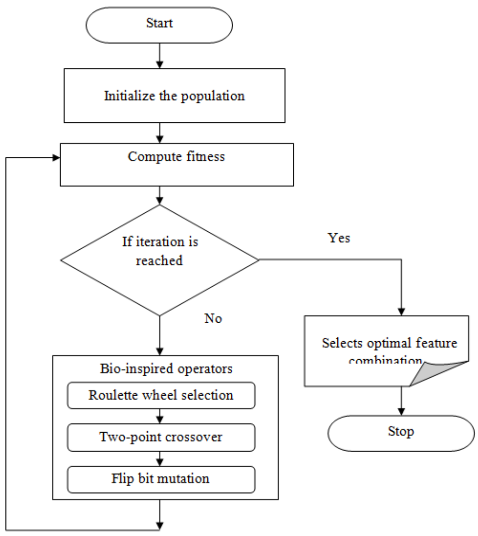

FIGURE 6: FLOW CHART OF THE STOCHASTIC ROULETTE GENE OPTIMIZATION

Figure 6 shows the flow chart of the proposed stochastic roulette gene optimizationto get the optimal feature combination. Initialize the populations of the feature combinations. For each individual, the fitness criterion is verified based on the error value. If the iteration is not met, then the roulette wheel selection, two-point crossover, and flip bit mutation are carried out to find the optimal solution. Then the fitness is verified again and the process gets iterated until it reaches the termination condition. Finally, the optimal feature combination is attained. After that, the features are estimated as given below,

TEXTURE FEATURE

The texture feature provides information about the spatial representation of pixels intensities which are evaluated as follows,

$$T_x = \frac{\sum_i \sum_j (p_i - m_i)(p_j - m_j)}{\sigma_i * \sigma_j} \quad (11)$$

Where, $T_x$indicates the texture feature, m_i, and m_j denote a mean of the pixels p_i, p_j, and their deviations are σ_i and σ_j.

INTENSITY

The intensity of the image is estimated as the difference between pixels and their neighboring pixels in an image. Consequently, the intensity of pixels are measured as given below,

$$Int = \sum_i \sum_j \left\| p_i - p_j \right\|^2 \quad (12)$$

Where Int indicates the intensity of the pixels p_i and their neighboring pixels p_j. Finally, the color feature from the input image is measured by converting the RGB color space into the HSV (hue, saturation, value).

$$m_{hsv} = \frac{1}{n} * Int \quad (13)$$

Where m_{hsv} designates the mean, Int denotes the intensity of pixels, n indicates the total number of pixels in an input satellite image. With the mean value, the variance is measured as follows,

$$\sigma^2{}_{hsv} = \frac{1}{n} \sum (Int - m_{hsv})^2 \quad (14)$$

Where $\sigma^2{}_{hsv}$ designates the variance, Indicates the intensity of pixel, m_{hsv} indicates a mean of HSV. Finally, the skewness is measured as follows,

$$\varphi_f = \frac{\frac{1}{n} \sum (Int - m_{hsv})^3}{\left(\frac{1}{n} \sum (Int - m_{hsv})^2\right)^{3/2}} \quad (15)$$

Where φ_f denotes the skewness. Based on the above-said mean, variance, and skewness, the color features are extracted.

// Algorithm 2 Stochastic roulette gene optimization based feature selection
Input: preprocessed image $L_1, L_2, L_3 \ldots .. L_n$ **Output**: Select and extract the features
Begin 1. Initialize the population of feature combination $W_i = C_1, C, C_3, \ldots . C_m$ 2. **for each** $C_i \in W_i$ 3. Calculate the fitness using (9) 4. **if** (stopping condition is met) **then** 5. Selects an optimal combination having less error 6. **else** 7. Select the individual from population-based fitness probability using (10) 8. Generate new offspring using a two-point crossover 9. Perform flip bit mutation 10. Replace old individual into a new one 11. Go to step 3 12. **End if** 13. **End for** 14. Extract the texture features T_x, 15. Extract the intensity features Int, 16. Extract the color features $m_{hsv}, \sigma^2{}_{hsv}, \varphi_f$ **End**

The above algorithm 2 describes the process of stochastic roulette gene optimization based feature selectionto find the fittest features for change detection with minimum time. Initially, the combination of the features is randomly initialized. Then the fitness of each individual is measured based on the error value. If the condition is not met, the various operators are used to find an optimal solution. Initially, the roulette wheel selection process is carried out to choose the individual from the population according to the fitness probability. With the selected individual, the recombination process is carried out to generate a new offspring. Finally, the flip bit mutation is performed to change the bit. After mutating the bits, the fitness function is measured with the newly generated individual. This process gets iterated until the condition is met. Then the selected features are given to the next process to minimize the time consumption.

3.3 DEEP JACCARD REGRESSIVE SQUEEZENET CONVOLUTIONAL STRUCTURE LEARNING

Finally, the extracted fittest features are then fed as input to the Deep Jaccard Regressive Squeezenet Convolutional Structure learning (DJRSCSL) architecture to detect the changes in remote sensing images. A DJRSCSL is a part of the machine learning technique and the word "deep" in deep learning indicates the use of multiple layers in the network to progressively analyze the higher-level features from the raw input images. The DJRSCSL designates that the network uses the mathematical process named convolution. SqueezeNet convolutional deep structure learning consists of an input and an output layer, and various hidden layers. On the contrary to the existing deep learning method, the Jaccard index Regression is applied in the hidden layer to minimize the change detection time. The architecture of Deep Jaccard Regressive Squeezenet Convolutional Structure learning is illustrated in figure 7.

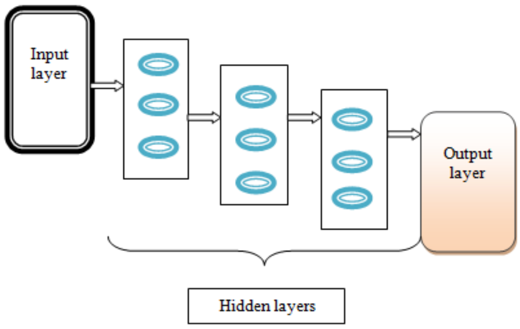

FIGURE 7: ARCHITECTURE OF DEEP JACCARD REGRESSIVE SQUEEZENET CONVOLUTIONAL STRUCTURE LEARNING

Figure 7 illustrates the architecture of Deep Jaccard Regressive Squeezenet Convolutional Structure learning with one input layer, three hidden layers, and one output layer. The input features are extracted and it was given to the input layer at a time 't'. Deep neural learning comprises the neurons-like the nodes are fully connected to the deep convolution layers with the adjustable weights. Then the inputs are transferred into the first hidden layer. Architecture is constructed by a stack of different hidden layers that transforms the input into output through a series of convolutional layers such as pooling layers, fully connected layers, and normalization layers.

At first, the input layer receives the features extracted from the satellite image into the network at a time 't' is denoted as '$x(t)$'. The activity of the neuron in the input and the weight value is denoted as follows,

$$X(t) = \sum_{i=1}^{q} h_i * x_i\,(t) + \beta \quad (16)$$

From (16), $X(t)$ indicates the activity of the neuron at the input layer, h_i denotes a weight which is a random number used to strengthen the connection between the layers, $x_i\ (t)$ indicates an input vector, β denotes a bias which is stored the value

is '+1'.

The input layer receives the number of input images and it is transformed into the first hidden layer. Hidden layers of a Deep Jaccard Regressive Squeezenet Convolutional Structure learning typically consist of a series of layers that convolve such as pooling layers, fully connected layers, and normalization layers. The first hidden layer is a pooling layer that helps to decrease the dimensions of the input by integrating the outputs of neurons at one layer into a single neuron in the consecutive layers. The second hidden layer in Deep Jaccard Regressive Squeezenet Convolutional is a fully connected layer which helps to link each neuron in one layer into subsequent layers. In the third hidden layer, the features mapping is performed using Jaccard Indexive Regression (JIR).JIR analysis is a set of statistical processes used for estimating the relationships between the features extracted from the different images.

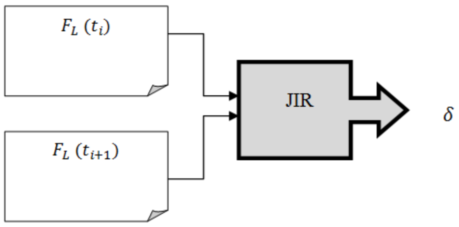

FIGURE 8: JACCARD INDEXIVE REGRESSION

Figure 8 illustrates the Jaccard Indexive Regression for mapping the features of the two homogeneous input images. Let us consider the features extracted from the input remote sensing image at a time t_i and t_{i+1} are $F_L\ (t_i)$ and $F_L\ (t_{i+1})$ respectively. The Jaccard similarity Index is expressed as follows,

$$H(t) = \delta = \frac{F_L\ (t_i) \cap F_L\ (t_{i+1})}{\sum F_L\ (t_i) + \sum F_L\ (t_{i+1}) - F_L\ (t_i) \cap F_L\ (t_{i+1})} \quad (17)$$

Where, $H(t)$ denotes an output of hidden layer, δ symbolizes Jaccard similarity coefficient, $F_L\ (t_i)$ signifies features extracted from the input remote sensing image at time t_i, $F_L\ (t_{i+1})$ indicates features extracted from the input remote sensing image at a time t_{i+1}, $F_L\ (t_i) \cap F_L\ (t_{i+1})$ is a mutual dependence between the features, $\sum F_L\ (t_i)$ is the sum of $F_L\ (t_i)$ score, $\sum F_L\ (t_{i+1})$ is the sum of $F_L\ (t_{i+1})$ score. The Jaccard similarity coefficient returns the output ranges from 0 to +1. Then the similarity values are sent to the output layer where the change detection is performed by setting the threshold value. The regression returns the similarity results by setting the threshold value as given below,

$$Y\ (t) = \begin{cases} \delta < T;\ less\ similarity \\ \delta > T;\ high\ similarity \end{cases} \quad (18)$$

Where $Y\ (t)$ denotes a deep learning output, T denotes a threshold. If the value of 'δ' is lesser than the threshold, then it is said to be less similarity i.e. the features of one image are varied from the other images. Otherwise, it returns high similarity i.e. the features of the one images are not varied from the images. In this way, the different changes in the two homogeneous images are correctly detected based on the feature mapping. Finally, the error rate (E) is measured based on the squared difference between the actual and predicted errors.

$$E = \left|E_a - E_p\right|^2 \quad (19)$$

Where E_a denotes an actual error, E_p indicates a predicted error. If the architecture attains the minimum error, then the process is stopped. Otherwise, the weight is adjusted and repeats the process until the error gets minimized. This helps for accurate change detection with minimum time.

// Algorithm 3:Deep Jaccard Regressive Squeezenet Convolutional Structure learning
Input: Extracted features **Output**: Increase change detection rate
Begin 1. **Given the** extracted features into **an** input layer $X(t)$ 2. Transform features into the first hidden layer to minimize the dimensions 3. Transform features into the second hidden layer 4. **For** the extracted feature $F_L\ (t_i)$ 5. **For** the extracted feature $F_L\ (t_{i+1})$ 6. Measure Jaccard similarity Index 'δ' at the third hidden layer 7. **If** ($\delta < T$)**then** 8. $Y\ (t)$ returns less similarity 9. Changes are detected 10. **Else** 11. $Y\ (t)$ returns a high similarity 12. Changes are not detected 13. **End if** 14. **End for** 15. **End for**

16. Measure error E
17. **If an error is not minimal then**
18. Update the weights Δh_i
19. Repeat the process
20. **End if**

End

The algorithmic process of the proposed is clearly described to detect the changes in the different input images. Initially, the extracted features are given to the input layer. Then it transforms into the hidden layers for mapping. The feature mapping process is carried out by using the Jaccard indexive regression function. The threshold is set to analyze the similarity value for identifying the changes. If the similarity value is lesser than the threshold, then the changes are correctly detected. Followed by an error rate is measured. The weights are updated and repeat the process until it reaches the minimum error to minimize the false positive rate.

4.EXPERIMENTAL EVALUATION AND PARAMETER DESCRIPTION

The experimental evaluation of the proposed SFSGO-DJRSCSL technique and existing methods namely SiamCRNN [1], IFN [2] are implemented using Keras python library high-level python API which is used to quickly build and train neural networks using Tensorflow as back-end. Keras is the lightweight framework that reduces the time complexity. The input satellite images are collected from the National Remote Sensing Centre (NRSC), ISRO (http://bhuvan.nrsc.gov.in). Bhuvan is an Indian web-based service that permits the users to examine a set of map-based content organized by the Indian Space Research Organization (ISRO).ISRO has used data provided by satellites comprising the Resourcesat-1, Cartosat-1, and Cartosat-2 to get the best feasible images of land cover.

The input homogeneous remote sensing images are collected and then perform the preprocessing. After the image preprocessing, the texture, intensity, and color features are extracted from the homogeneous images. Finally, Deep Jaccard Regressive Squeezenet Convolutional Structure learning is used to map the extracted features from the homogeneous images and detect the different changes using the Jaccard similarity index value. The performance of the proposed SFSGO-DJRSCSL technique is analyzed with the existing methods using different performance metrics such as detection rate, false alarm rate, and detection time.

4.1 QUALITATIVE ANALYSIS

In this section, a qualitative analysis of the proposed SFSGO-DJRSCSL technique is illustrated with different processes.

	Satellite band image 1 at 22mar2015	Satellite band image 1 at 16Apr2017

Original band image		
After Preprocessing		
Feature detection and extraction	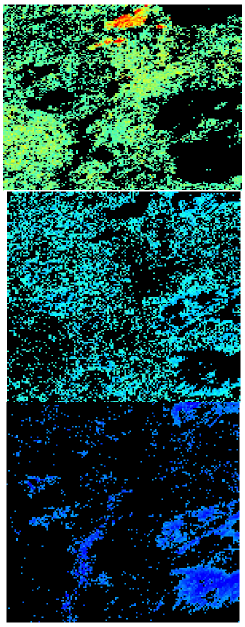	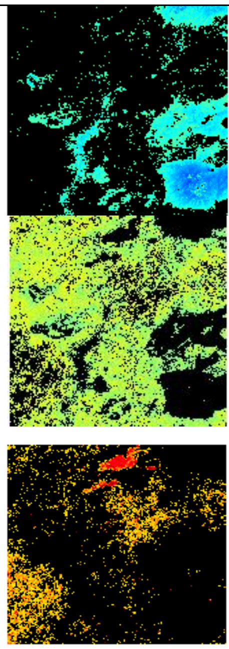
Change detection	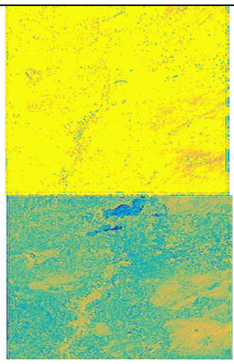	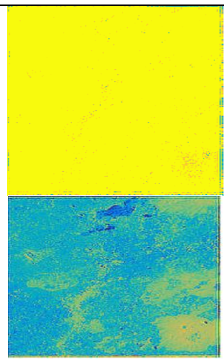

FIGURE 9: QUALITATIVE RESULTS OF SFSGO-DJRSCSL TECHNIQUE

Figure 9 given above depicts the qualitative results of the SFSGO-DJRSCSL technique. Initially, the pair of band images are collected and the preprocessing is carried out such as radiometric correction,atmospheric corrections, topographic correction, and contrast enhancement. After obtaining the preprocessed image, texture, intensity, and color features are extracted from the pair of band images. Finally, the extracted features from the two images are matched using Deep Jaccard Regressive Squeezenet Convolutional network. The two images' features are less similar and the changes are accurately detected.

4.2. QUANTITATIVE ANALYSIS

In this section, the quantitative analysisof the proposed SFSGO-DJRSCSL technique and the two related methods namely SiamCRNN [1], IFN [2] are evaluated with various quantitative metrics such as detection rate, false alarm rate, and detection time. These metrics are described in this section.

DETECTION RATE

Detection rate is measured as the changes in the given input images are correctly identified by an algorithm to the total number of images taken as input. The Detection rate is calculated using a given formula,

$$DR = \left(\frac{changes\ in\ images\ are\ correctly\ detected}{n}\right) * 100 \quad (20)$$

Where DR denotes a detection rate, n represents the number of images. The detection rate is measured in the unit of percentage (%).

FALSE ALARM RATE

False alarm rateis measured as the changes in the given input images are incorrectly identified by an algorithm to the total number of images taken as input. The False alarm rateis calculated using a given formula,

$$FAR = \left(\frac{changes\ in\ images\ are\ incorrectly\ detected}{n}\right) * 100 \quad (21)$$

Where FAR denotes a false alarm rate, n represents the number of images. The False positive rateis measured in the unit of percentage (%).

DETECTION TIME

Detection timeis defined as the amount of time taken by an algorithm to detect the changes in the homogeneous images. The detection timeis calculated mathematically as given below,

$$DT = n * time\ \ (DC_s) \quad (22)$$

Where DT denotes a detection time, n represents the number of images, DC_s denotes a time taken for change detection using one pair of images. The detection timeis measured in the unit of milliseconds (ms).

Table I Comparison of detection rate

Band image pairs	Detection rate (%)		
	SFSGO-DJRSCSL	SiamCRNN	IFN

(numbers)			
5	80	60	60
10	80	70	60
15	87	80	73
20	85	80	75
25	88	84	76
30	90	83	80
35	91	86	83
40	90	85	80
45	91	84	80
50	92	88	84

Table I indicates performance results of change detection rate for the number of band image pairs collected from different years. 50 combinations of images are collected with different years of images from the same geographic location. Ten different runs are obtained for each technique. As shown in Table I, 5 pair of band images are considered for performing change detection. By applying the SFSGO-DJRSCSL technique, 80% of change detection is observed. Similarly, 60% of the change detection rates are observed by applying the SiamCRNN [1], IFN [2]. Further, to evaluate the performance of the SFSGO-DJRSCSL technique, a comparison is made between the results achieved with [1] [2]. The average comparison of ten results indicates that the SFSGO-DJRSCSL technique outperforms well than the other two methods and it achieves a higher detection rate by 10% when compared to [1] and 17% when compared to [2].

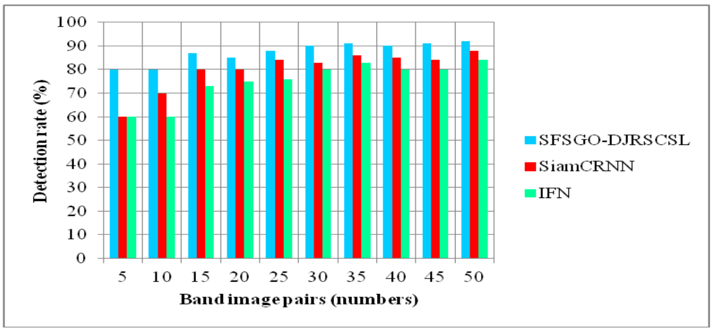

FIGURE 10: GRAPHICAL ILLUSTRATION OF DETECTION RATE

Figure 10 illustrates a visual comparison of the change detection performance achieved with the three different techniques. The graphical illustration shows that the numbers of band image pairs are given as input 'x' direction and the performance of change detection rate is observed at 'y' direction. The change detection rates of three different techniques SFSGO-DJRSCSL technique, SiamCRNN [1], IFN [2] are observed in three different colors namely blue, red, and green respectively. The graph shows that the performance of the change detection rate is comparatively higher than the other existing methods. This means that the SFSGO-DJRSCSL technique uses the Deep Jaccard Regressive Squeezenet Convolutional Structure learning to detect the changes between two homogeneous band images by mapping the features. The Jaccard similarity performs feature mapping. If both features are correctly matched, there is no changes were made. Otherwise, the changes are detected with higher accuracy.

Table II Comparison of False alarm rate

Band image pairs (numbers)	False alarm rate (%)		
	SFSGO-DJRSCSL	SiamCRNN	IFN
5	20	40	40
10	20	30	40
15	13	20	27
20	15	20	25
25	12	16	24
30	10	17	20
35	9	14	17
40	10	15	20
45	9	16	20
50	8	12	16

Table II illustrates the quantitative analysis of the false alarm rate of three different techniques versus the number of band images. The above results indicate that the false alarm rate is minimized in the change detection using the SFSGO-DJRSCSL technique than the existing approaches. The results of the SFSGO-DJRSCSL technique is compared to the performance results of SiamCRNN [1], IFN [2]. The comparison results prove that an average of ten results shows that the false alarm rate is significantly reduced by 36% and 49% when compared to existing [1] [2] respectively.

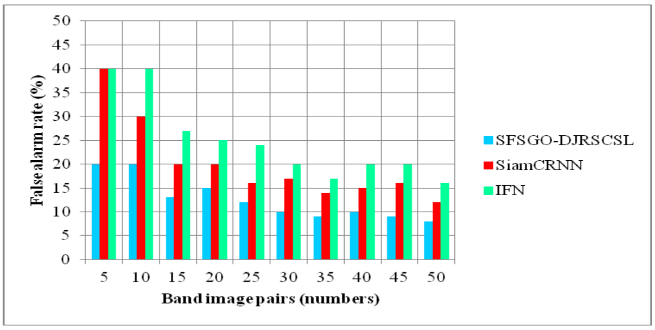

FIGURE 11: GRAPHICAL REPRESENTATION OF FALSE ALARM RATE

Figure 11 depicts the performance of the false alarm rate for the number of band image pairs. The above figure allows a visual comparison of the change detection performance achieved with the three different techniques. The above figure shows that the false alarm rate is considerably minimized and obtaining a higher detection rate using the SFSGO-DJRSCSL technique than the other existing methods. This improvement is achieved through the deep learning concept. The Jaccard Regression function analyzes the features based on the similarity measure. If the two features are having a lesser similarity than the threshold, then the changes are accurately detected. Besides, the deep learning process accurately analyzes the features and displays feature matching results at the output layer.

Table III Comparison of detection time

Band image pairs (numbers)	Detection time (ms)		
	SFSGO-DJRSCSL	SiamCRNN	IFN
5	12	14	16
10	18	20	22
15	23	26	29
20	26	28	30
25	28	30	33
30	32	35	37
35	36	39	42
40	40	43	46
45	43	46	50
50	46	50	55

Table III illustrates the detection time versus band images using three different change detection techniques. The quantitative comparison analysis shows that the detection time estimation is considerably better than the existing change detection techniques. This is proved by the statistical evaluation by considering 5 input band images. The detection time of the SFSGO-DJRSCSL technique is obtained as $12ms$ and the detection time of the other two methods SiamCRNN [1], IFN [2] are observed as $14ms$ and $16ms$ respectively. Similarly, the remaining runs are carried out and the results are compared. The comparison results of the ten different results indicate that the SFSGO-DJRSCSL technique reduces the change detection time by 9% and 16% when compared to SiamCRNN [1], IFN [2] respectively.

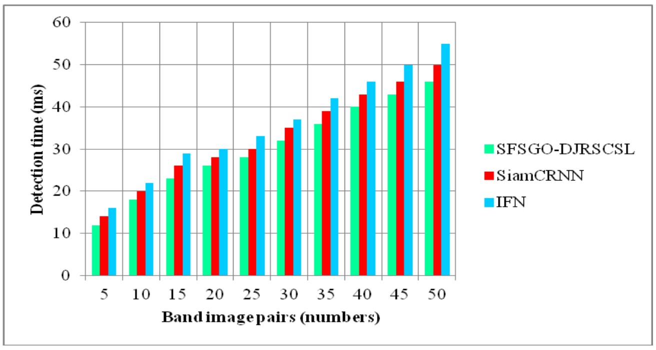

FIGURE 12: GRAPHICAL REPRESENTATION OF DETECTION TIME

Figure 12 depicts the convergence graph of detection time with the increasing counts of the number of band image pairs. Compared to other existing methods, the SFSGO-DJRSCSL technique minimizes the detection time than the other methods. This is due to the application of preprocessing and feature extraction. The input homogeneous satellite band images are collected from the database. For each input band image, preprocessing such as radiometric normalization, atmospheric correction, topographic correction, contrast enhancement are performed to obtain the quality enhanced image for accurate change detection with minimum time consumption. Besides, the stochastic roulette gene optimization based feature selection is carried out to find the survival of the fittest features. Followed by, the change detection resulting in it minimizes the time consumption. Then the feature mapping is carried out in the deep learning process.

5. CONCLUSION

In this article, a novel technique called SFSGO-DJRSCSL technique is proposed for change detection in homogeneous VHR images with a different period. The SFSGO-DJRSCSL technique consists of three sub-processes namely preprocessing, feature detection, and extraction and the final one is a classification. The first part of the SFSGO-DJRSCSL technique is preprocessing which performing the various corrections from the given input image to obtain the quality enhanced image for accurate change detection and minimizing time consumption. Followed by, the optimal fittest feature combinations are detected and extract spatial-spectral features from the image. Finally, the two features from the homogeneous images are mapped using a new latent feature space using Deep Jaccard Regressive Squeezenet Convolutional Structure learning, and abundant change information is generated based on the similarity value. The comprehensive experimental assessment is conducted and the quantitative, as well as qualitative performance analysis, is performed with different metrics. The quantitative results indicate that the SFSGO-DJRSCSL technique outperforms in terms of achieving a higher detection rate and lesser time as well as a false alarm rate when compared to other related methods..

REFERENCES

[1] Hongruixuan Chen, Chen Wu, Bo Du, Liangpei Zhang, Le Wang, "Change Detection in Multisource VHR Images via Deep Siamese Convolutional Multiple-Layers Recurrent Neural Network", IEEE Transactions on Geoscience and Remote Sensing, Volume 58, Issue 4, 2020, Pages 2848 -2864

[2] Chenxiao Zhang, Peng Yueb, Deodato Tapete, Liangcun Jiang, Boyi Shangguan, Li Huang, Guangchao Liu, "A deeply supervised image fusion network for change detection in high resolution bi-temporal remote sensing images", ISPRS Journal of Photogrammetry and Remote Sensing, Volume 166, 2020, Pages 183-200

[3] Saurabh Kumar, Shwetankb, Kamal Jain, "A Multi-Temporal Landsat Data Analysis for Land-use/Land-cover Change in Haridwar Region using Remote Sensing Techniques", Procedia Computer Science, Elsevier, Volume 171, 2020, Pages 1184-1193

[4] Sudipan Saha, Francesca Bovolo, Lorenzo Bruzzone, "Unsupervised Deep Change Vector Analysis for Multiple-Change Detection in VHR Images", IEEE Transactions on Geoscience and Remote Sensing, Volume 57, Issue 6, 2019, Pages 3677 – 3693

[5] Xin Huanga, Yinxia Caoa, Jiayi Lia, "An automatic change detection method for monitoring newly constructed building areas using time-series multi-view high-resolution optical satellite images", Remote Sensing of Environment, Elsevier, Volume 244, 2020, Pages 1-18

[6] Redha Touati, Max Mignotte, Mohamed Dahmane, "Multimodal Change Detection in Remote Sensing Images Using an Unsupervised Pixel Pairwise Based Markov Random Field Model", IEEE Transactions on Image Processing, Volume 29, 2019, Pages 757 – 767

[7] Neha Gupta, Gargi V. Pillai, and Samit Ari, "Change Detection in Optical Satellite Images Based on Local Binary Similarity Pattern Technique", IEEE Geoscience and Remote Sensing Letters, Volume 15, Issue 3, 2018, Pages 389 – 393

[8] Neelam Ruhil, Mohan Singh, Debjani Mitra, Akansha Singh, Krishna Kant Singh, "Detection of changes from Satellite Images Using Fused Difference Images and Hybrid Kohonen Fuzzy C-Means Sigma", Procedia Computer Science, Elsevier, Volume 167, 2020, Pages 431-439

[9] Wenping Ma, Yunta Xiong, Yue Wu, Hui Yang, Xiangrong Zhang, and Licheng Jiao, "Change Detection in Remote Sensing Images Based on Image Mapping and a Deep Capsule Network", Remote Sensing, Volume 11, 2019, Pages 1-24

[10] Akansha Singh and Krishna Kant Singh, "Unsupervised change detection in remote sensing images using a fusion of spectral and statistical indices", The Egyptian Journal of Remote Sensing and Space Sciences, Elsevier, Volume 21, 2018, Pages 345-351

[11] Li Yan, Wang Xia, Zhan Zhao, and Yanran Wang, "A Novel Approach to Unsupervised Change Detection Based on Hybrid Spectral Difference", Remote Sensing, Volume 10, 2018, Pages 1-21

[12] Wenqiang Xi, Shihong Du, Yi-Chen Wang, Xiuyuan Zhang, "A spatiotemporal cube model for analyzing satellite image time series: Application to land-cover mapping and change detection", Remote Sensing of Environment, Elsevier, Volume 231, 2019, Pages 1-22

[13] Hui Luo, Chong Liu, Chen Wu, and Xian Guo, "Urban Change Detection Based on Dempster–Shafer Theory for Multitemporal Very High-Resolution Imagery", Remote Sensing, Volume 10, Issue 7, 2018, Pages 1-18

[14] Lichao Mou, Lorenzo Bruzzone, and Xiao Xiang Zhu, "Learning Spectral-Spatial-Temporal Features via a Recurrent Convolutional Neural Network for Change Detection in Multispectral Imagery", IEEE Transactions On Geoscience And Remote Sensing, Volume 57, Issue 2, 2019, Paged 924-935

[15] Xudong Niu, Maoguo Gong, Tao Zhan, Yuelei Yang, "A Conditional Adversarial Network for Change Detection in Heterogeneous Images", IEEE Geoscience and Remote Sensing Letters Volume 16, Issue 1, 2019, Pages 45 – 49

[16] Jia Liu, Maoguo Gong, Kai Qin, Puzhao Zhang, "A Deep Convolutional Coupling Network for Change Detection Based on Heterogeneous Optical and Radar Images", IEEE Transactions on Neural Networks and Learning Systems, Volume 29, Issue 3, 2018, Pages 545 – 559

[17] Jia Liu, Maoguo Gong, A. K. Qin, Kay Chen Tan, "Bipartite Differential Neural Network for Unsupervised Image Change Detection". IEEE Transactions on Neural Networks and Learning Systems, Volume 31, Issue 3, 2020, Pages 876 – 890

[18] Suicheng Li, Pengcheng Han, Shuhui Bu, Pinmo Tong, Qing Li, Ke Li, Gang Wan, "Change detection in images using shape-aware siamese convolutional network", Engineering Applications of Artificial Intelligence, Elsevier, Volume 94, 2020, Pages 1-11

[19] José A. Padrón-Hidalgo, Valero Laparra, Nathan Longbotham, Gustau Camps-Valls, "Kernel Anomalous Change Detection for Remote Sensing Imagery", IEEE Transactions on Geoscience and Remote Sensing, Volume 57, Issue 10, 2019, Pages 7743 – 7755

[20] Zhi Li, Zhenhong Jia, luyang liua, Jie Yanga, Nikola Kasabov, "A method to improve the accuracy of SAR image change detection by using an image enhancement method", ISPRS Journal of Photogrammetry and Remote Sensing, Elsevier, Volume 163, 2020, Pages 137-151.